RDECOM TR 10-D-113

**U.S. ARMY RESEARCH,
DEVELOPMENT AND
ENGINEERING COMMAND**

TITLE: The S415 and S418 Airfoils

AUTHOR: **Dan M. Somers**

COMPANY NAME: **Airfoils, Incorporated**

COMPANY ADDRESS: **122 Rose Drive
Port Matilda PA 16870-7535**

DATE: **August 2010**

FINAL REPORT: **Contract Number W911W6-07-C-0047, SBIR Phase II,
Topic Number A06-006, Proposal Number A2-2972**

Prepared for:

U.S. ARMY RESEARCH, DEVELOPMENT AND ENGINEERING COMMAND, AVIATION APPLIED TECHNOLOGY DIRECTORATE, FORT EUSTIS, VA 23604-5577

AIRFOILS, INCORPORATED
122 ROSE DRIVE
PORT MATILDA, PA 16870-7535 USA
WEBSITE WWW AIRFOILS.COM
TELEPHONE (814) 357-0500
FACSIMILE (814) 357-0357

THE S415 AND S418 AIRFOILS

DAN M. SOMERS

AUGUST 2010

ABSTRACT

Two, 14.1-percent-thick, natural-laminar-flow airfoils, the S415 and S418, intended for the blade of a slowed-rotor helicopter have been designed and analyzed theoretically. The S415 airfoil, designed for the hover condition, is "unmorphed" into the S418 airfoil, which is more suitable for forward flight. The two primary objectives of high maximum lift and low profile drag have been achieved. The constraints on the pitching moments have been satisfied.

INTRODUCTION

Almost all airfoils in use on rotorcraft today were developed under the assumption that extensive laminar flow is not likely on a rotor. (See ref. 1, for example.) For the present application, however, given the moderate Reynolds numbers and the exploratory nature of the study, the achievement of laminar flow warrants examination.

The two airfoil shapes designed under the study are intended for the blade of a slowed-rotor helicopter. The airfoil was initially designed for the hover condition and then "unmorphed" into a shape more suitable for forward flight. (See ref. 2.) To complement the design study, an investigation was conducted in The Pennsylvania State University Low-Speed, Low-Turbulence Wind Tunnel to obtain the basic, low-speed, two-dimensional aerodynamic characteristics of the hover configuration (ref. 3). These airfoil shapes are part of an effort sponsored by the U.S. Army to design theoretically and verify experimentally several airfoils for rotorcraft applications.

SYMBOLS

C_p	pressure coefficient
c	airfoil chord, mm (in.)
c_d	section profile-drag coefficient
c_l	section lift coefficient
c_m	section pitching-moment coefficient about quarter-chord point
M	free-stream Mach number
R	Reynolds number based on free-stream conditions and airfoil chord
t	airfoil thickness, mm (in.)
x	airfoil abscissa, mm (in.)

α angle of attack relative to x-axis, deg

Subscripts:

dd drag divergence

ll lower limit of low-drag range

max maximum

min minimum

S separation

T transition

ul upper limit of low-drag range

0 zero lift

Abbreviations:

L. lower surface

S. boundary-layer separation location, x_S/c

T. boundary-layer transition location, x_T/c

U. upper surface

AIRFOIL DESIGN

OBJECTIVES AND CONSTRAINTS

The airfoil design specifications are contained in table I. Two primary objectives are evident for the hover configuration (table I(a)). The first objective is to achieve a maximum lift coefficient of 1.50 at a Mach number of 0.50 and a Reynolds number of 5.00×10^6. A requirement related to this objective is that the maximum lift coefficient not decrease significantly with transition fixed near the leading edge on both surfaces. In addition, the airfoil should exhibit docile stall characteristics at a Mach number of 0.2 and a Reynolds number of 2.0×10^6, which is within the operational range of The Pennsylvania State University Low-Speed, Low-Turbulence Wind Tunnel. The second objective is to obtain low profile-drag coefficients over the range of lift coefficients from 0.60 to 1.40 at a Mach number of 0.50 and a Reynolds number of 5.00×10^6. One major constraint was placed on the design: At a Mach

number of 0.40 and a Reynolds number of 4.00×10^6, the pitching-moment coefficient at a lift coefficient of 1.50 must be no more negative than –0.10.

Two primary objectives are evident for the forward-flight configuration (table I(b)). The first objective is to achieve a maximum lift coefficient of 0.80 at a Mach number of 0.60 and a Reynolds number of 6.00×10^6. A requirement related to this objective is that the maximum lift coefficient not decrease significantly with transition fixed near the leading edge on both surfaces. In this configuration, the airfoil is not expected to exceed the maximum lift coefficient and, therefore, the stall characteristics are irrelevant. The second objective is to obtain low profile-drag coefficients over the range of lift coefficients from 0.02 to 0.10 at a Mach number of 0.70 and a Reynolds number of 7.00×10^6. Two major constraints were placed on this configuration: First, at a Mach number of 0.72 and a Reynolds number of 7.20×10^6, the zero-lift pitching-moment coefficient must be no more negative than –0.02; second, the airfoil thickness must equal that of the hover configuration (i.e., the midchord region of the airfoil does not morph).

PHILOSOPHY

Given the above objectives and constraints, certain characteristics of the designs are apparent. The following sketch illustrates a drag polar that meets the goals for the hover configuration.

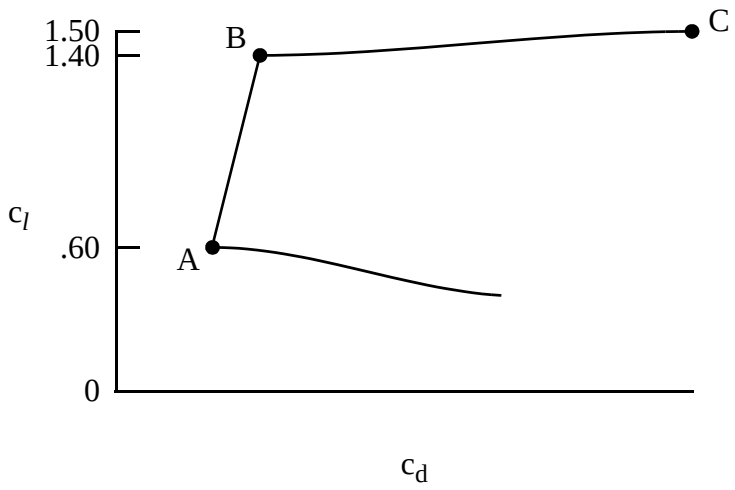

Sketch 1

The desired airfoil shape can be traced to the pressure distributions that occur at the various points in sketch 1. Point A is the lower limit of the low-drag range of lift coefficients; point B, the upper limit. The profile-drag coefficient at point B is not as low as at point A, unlike the

polars of many laminar-flow airfoils where the drag coefficient within the laminar bucket is nearly constant. (See, for example, ref. 4.) This characteristic is related to the elimination of significant (i.e., drag-producing) laminar separation bubbles on the upper surface for the design Reynolds number. (See ref. 5.) The drag coefficient increases rapidly outside the low-drag, lift-coefficient range because boundary-layer transition moves quickly toward the leading edge with increasing (decreasing) lift coefficient. This feature results in a leading-edge shape that produces a suction peak at higher lift coefficients, which ensures that transition on the upper surface will occur very near the leading edge. Thus, the maximum lift coefficient, point C, occurs with turbulent flow along the entire upper surface and, therefore, should be relatively insensitive to roughness at the leading edge.

From the preceding discussion, the pressure distributions along the polar can be deduced. The pressure distribution at point A should look something like sketch 2.

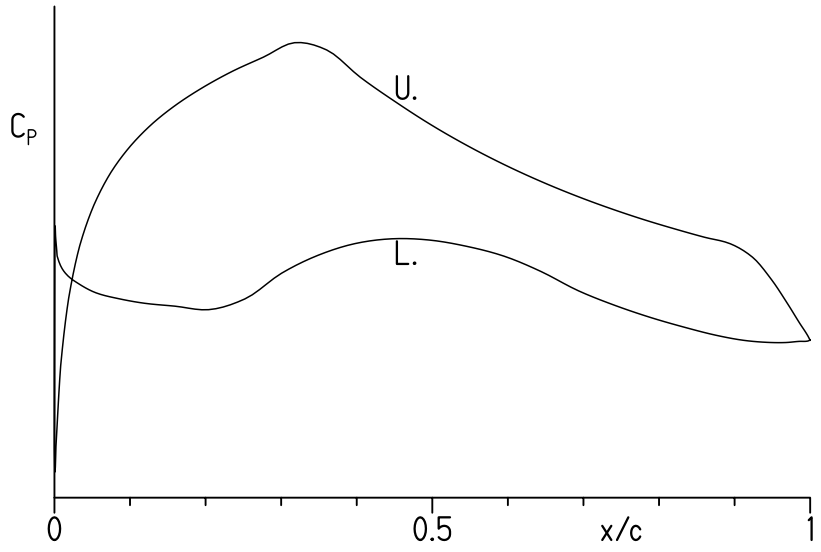

Sketch 2

To achieve low drag, a favorable pressure gradient is desirable along the upper surface to about 30-percent chord. Aft of this point, a short region having a shallow, adverse pressure gradient (i.e., a “transition ramp”) promotes the efficient transition from laminar to turbulent flow (ref. 6). The transition ramp is followed by a concave pressure recovery, which exhibits lower drag and has less tendency to separate than the corresponding linear or convex pressure recovery (ref. 6). The specific pressure recovery employed represents a compromise between maximum lift, drag, pitching moment, stall characteristics, and drag divergence. The steep, adverse pressure gradient aft of about 90-percent chord is a “separation ramp,” originally proposed by F. X. Wortmann,[1] which confines turbulent separation to a small region near the trailing edge. By constraining the movement of the separation point at high angles of attack,

higher lift coefficients can be achieved with little drag penalty. (See ref. 7.) This feature has the added benefit of promoting docile stall characteristics. (See ref. 8.)

Along the lower surface, the pressure gradient is initially adverse and then favorable to about 45-percent chord. Thus, transition is imminent over the forward portion of the lower surface. (See ref. 9.) This concept allows a wide low-drag range to be achieved and increases the loading in the leading-edge region. The forward loading serves to balance, with respect to the pitching-moment constraint, the aft loading, both of which contribute to the achievement of a high maximum lift coefficient and low profile-drag coefficients. This region is followed by a transition ramp and then a concave pressure recovery.

The amounts of pressure recovery on the upper and lower surfaces are determined by the width of the low-drag, lift-coefficient range and the pitching-moment constraint.

At point B, the pressure distribution should look like sketch 3.

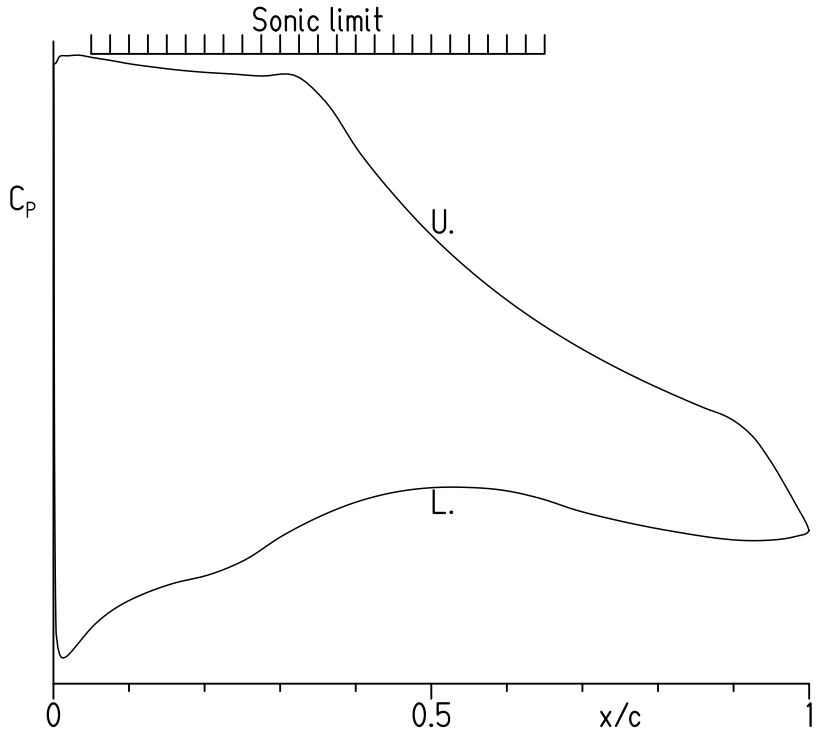

Sketch 3

[1]Director, Institute for Aerodynamics and Gas Dynamics, University of Stuttgart, Germany, 1974–1985.

No suction peak exists at the leading edge. Instead, a moderately adverse pressure gradient extends from the leading edge to the beginning of the pressure recovery.

EXECUTION

Given the pressure distributions previously discussed, the design of the airfoil in the hover configuration is reduced to the inverse problem of transforming the pressure distributions into an airfoil shape. The Eppler Airfoil Design and Analysis Code (refs. 10 and 11) was used because of its unique capability for multipoint design and because of confidence gained during the design, analysis, and experimental verification of many other airfoils. (See ref. 12, for example.) The airfoil in the hover configuration is designated the S415. The airfoil shape for forward flight was derived by deflecting the leading- and trailing-edge regions upward. The airfoil in the forward-flight configuration is designated the S418. The airfoil shapes and coordinates are available from Airfoils, Incorporated. The airfoil thickness is 14.1-percent chord.

THEORETICAL PROCEDURE

The results are predicted using the method of references 10 and 11 (PROFIL07), commonly known as the Eppler code, and the method of reference 13 (MSES 3.0). Critical amplification factors of 11 and 9 were specified for the boundary-layer transition computations using the method of references 10 and 11 and the method of reference 13, respectively. Because the maximum lift coefficient computed by the method of references 10 and 11 is not always realistic, an empirical criterion has been applied to the computed results. The criterion assumes the maximum lift coefficient has been reached if the drag coefficient of the upper surface reaches a certain value that is a function of the Reynolds number and the wind-tunnel facility. It should also be noted that the compressibility correction (ref. 14) incorporated in the method of references 10 and 11 is invalid if the local flow is supersonic.

Computations were performed over the range of operational conditions in table I with transition free (smooth) and with transition fixed near the leading edge, 2-percent chord on the upper surface and 5-percent chord on the lower surface, to simulate full-chord, turbulent flow.

DISCUSSION OF RESULTS

S415 AIRFOIL

Pressure Distributions

The pressure distributions for the S415 airfoil predicted using the method of reference 13 at various angles of attack at a Mach number of 0.50 and a Reynolds number of 5.00×10^6 with transition free are shown in figure 1. At an angle of attack of 0.00° (fig. 1(a)), a short laminar separation bubble is evident on the upper surface around 40-percent chord and

on the lower surface just aft of the leading edge. At an angle of attack of 1.00° (fig. 1(a)), the bubble on the lower surface has jumped aft to around 60-percent chord. As the angle of attack is increased, the bubble on the upper surface migrates slowly forward and the one on the lower surface, slowly aft (figs. 1(a)–1(c)). At an angle of attack of 7.00° (fig. 1(c)), the flow over the forward 20-percent chord of the upper surface is supersonic. At an angle of attack of 8.00° (fig. 1(c)), despite significant supersonic flow, no wave drag or turbulent, trailing-edge separation is predicted.

Section Characteristics

The section characteristics of the S415 airfoil at a Mach number of 0.50 and a Reynolds number of 5.00×10^6 with transition free predicted using the method of references 10 and 11 (PROFIL07) and the method of reference 13 (MSES 3.0) are shown in figure 2. The results are in reasonably good agreement. (It should be remembered that the compressibility correction incorporated in the method of refs. 10 and 11 is invalid if the local flow is supersonic and, accordingly, only subsonic results are shown.) The method of reference 13 generally predicts lower profile-drag coefficients. The method predicts a maximum lift coefficient that exceeds the design objective of 1.50. The method of references 10 and 11 predicts the lower limit of the low-drag, lift-coefficient range meets the objective, but the upper limit is below the objective of 1.40. Conversely, the method of reference 13 predicts the lower limit is above the objective of 0.60, but the upper limit exceeds the objective. Neither method confirms the objective for the minimum lift coefficient, 0.40, can be achieved. At a Mach number of 0.40 and a Reynolds number of 4.00×10^6, the method of reference 13 predicts the pitching-moment coefficient at a lift coefficient of 1.50 is –0.10, which satisfies the design constraint.

The effect of fixing transition on the section characteristics is shown in figure 3. The lift-curve slope, the maximum lift coefficient, and the magnitude of the pitching-moment coefficients decrease with transition fixed. These results are a consequence of the boundary-layer displacement effect, which decambers the airfoil because the displacement thickness is greater with transition fixed than with transition free. In addition, the lift coefficient decreases with transition fixed because the roughness induces earlier trailing-edge separation. (See fig. 3(a).) The reduction in maximum lift coefficient is 3 percent. The drag coefficients are, of course, adversely affected by fixing transition.

Based on the predictions, all the design objectives and the design constraint for the S415 airfoil have essentially been met.

S418 AIRFOIL

Pressure Distributions

The pressure distributions for the S418 airfoil predicted using the method of reference 13 at various angles of attack at a Mach number of 0.60 and a Reynolds number of

6.00×10^6 with transition free are shown in figure 4. At an angle of attack of 0.00° (fig. 4(a)), a short laminar separation bubble is evident on the upper surface around 50-percent chord and on the lower surface around 55-percent chord. As the angle of attack is increased, the bubble on the upper surface moves forward and the bubble on the lower surface migrates slowly aft (figs. 4(a) and 4(b)). At an angle of attack of 4.00° (fig. 4(b)), the flow near the leading edge on the upper surface is supersonic, but no wave drag is predicted. At an angle of attack of 5.00° (fig. 4(b)), a shock is evident on the upper surface and significant wave drag is predicted.

The pressure distributions predicted at various angles of attack at a Mach number of 0.70 and a Reynolds number of 7.00×10^6 with transition free are shown in figure 5. At an angle of attack of 0.00° (fig. 5(a)), a short laminar separation bubble is evident on the upper surface around 45-percent chord and on the lower surface around 55-percent chord, just aft of a small supersonic region. At an angle of attack of 0.50° (fig. 5(a)), the flow over both surfaces is subsonic. As the angle of attack is increased, the bubble on the upper surface moves forward and the one on the lower surface migrates slowly aft (fig. 5(a)). At an angle of attack of 1.00° (fig. 5(a)), the flow over about 20 percent of the upper surface is supersonic. At an angle of attack of 2.00° (fig. 5(b)), despite significant supersonic flow, little wave drag and no turbulent, trailing-edge separation are predicted.

Section Characteristics

The section characteristics of the S418 airfoil with transition free at a Mach number of 0.60 and a Reynolds number of 6.00×10^6 and at a Mach number of 0.70 and a Reynolds number of 7.00×10^6 predicted using the method of references 10 and 11 (PROFIL07) and the method of reference 13 (MSES 3.0) are shown in figure 6. The results are in reasonable agreement. (Again, it should be remembered that only subsonic results are shown for the method of refs. 10 and 11.) The method of reference 13 generally predicts lower profile-drag coefficients, at least in part because it predicts transition farther aft. At a Mach number of 0.60 and a Reynolds number of 6.00×10^6 (fig. 6(a)), the method of reference 13 predicts a maximum lift coefficient that meets the design objective of 0.80. At a Mach number of 0.70 and a Reynolds number of 7.00×10^6 (fig. 6(b)), both methods predict a low-drag, lift-coefficient range that meets the design objective. At a Mach number of 0.72 and a Reynolds number of 7.20×10^6, the method of reference 13 predicts the zero-lift pitching-moment coefficient is 0.03, which surpasses the design constraint. The method predicts a drag-divergence Mach number of 0.73, which is below the design goal of 0.75.

The effect of fixing transition on the section characteristics is shown in figures 7 and 8. Neither method predicts significant effects, except on the drag coefficients.

Based on the predictions, all the design objectives for the S418 airfoil have essentially been met.

CONCLUDING REMARKS

Two, 14.1-percent-thick, natural-laminar-flow airfoils, the S415 and S418, intended for the blade of a slowed-rotor helicopter have been designed and analyzed theoretically. The S415 airfoil, designed for the hover condition, is "unmorphed" into the S418 airfoil, which is more suitable for forward flight. The two primary objectives of high maximum lift coefficients and low profile-drag coefficients have been achieved. The constraints on the pitching-moment coefficients have been satisfied.

ACKNOWLEDGMENTS

This effort was sponsored by the U.S. Army. Preston B. Martin served as the technical monitor.

REFERENCES

1. Noonan, Kevin W.: Aerodynamic Characteristics of Two Rotorcraft Airfoils Designed for Application to the Inboard Region of a Main Rotor Blade. NASA TP-3009, 1990.

2. Kota, Sridhar; Ervin, Gregory; Osborn, Russell; and Ormiston, Robert A.: Design and Fabrication of an Adaptive Leading Edge Rotor Blade. American Helicopter Soc. 64th Annual Forum, Montreal, Canada, April 29 – May 1, 2008.

3. Somers, Dan M.; and Maughmer, Mark D.: Design and Experimental Results for the S415 Airfoil. U.S. Army RDECOM TR 10-D-114, 2010. (Available from DTIC.)

4. Abbott, Ira H.; Von Doenhoff, Albert E.; and Stivers, Louis S., Jr.: Summary of Airfoil Data. NACA Rep. 824, 1945. (Supersedes NACA WR L-560.)

5. Eppler, Richard; and Somers, Dan M.: Airfoil Design for Reynolds Numbers Between 50,000 and 500,000. Proceedings of the Conference on Low Reynolds Number Airfoil Aerodynamics, UNDAS-CP-77B123, Univ. of Notre Dame, June 1985, pp. 1–14.

6. Wortmann, F. X.: Experimental Investigations on New Laminar Profiles for Gliders and Helicopters. TIL/T.4906, British Minist. Aviat., Mar. 1960. (Translated from Z. Flug-wissenschaften, Bd. 5, Heft 8, Aug. 1957, S. 228–243.)

7. Eppler, R.: Comparison of Theoretical and Experimental Profile Drags. NASA TT F-16981, 1976. (Translated from Schweizer Aero-Revue, vol. 38, no. 10, Oct. 1963, pp. 593–595.)

8. Maughmer, Mark D.; and Somers, Dan M.: Design and Experimental Results for a High-Altitude, Long-Endurance Airfoil. J. Aircr., vol. 26, no. 2, Feb. 1989, pp. 148–153.

9. Eppler, R.: Laminar Airfoils for Reynolds Numbers Greater Than 4×10^6. B-819-35, Apr. 1969. (Available from NTIS as N69-28178; translated from Ingenieur-Archiv, Bd. 38, Heft 4/5, 1969, S. 232–240.)

10. Eppler, Richard: Airfoil Design and Data. Springer-Verlag (Berlin), 1990.

11. Eppler, Richard: Airfoil Program System “PROFIL07.” User’s Guide. Richard Eppler, c.2007.

12. Somers, Dan M.: Subsonic Natural-Laminar-Flow Airfoils. Natural Laminar Flow and Laminar Flow Control, R. W. Barnwell and M. Y. Hussaini, eds., Springer-Verlag New York, Inc., 1992, pp. 143–176.

13. Drela, M.: Design and Optimization Method for Multi-Element Airfoils. AIAA Paper 93-0969, Feb. 1993.

14. Labrujere, Th. E.; Loeve, W.; and Sloof, J. W.: An Approximate Method for the Determination of the Pressure Distribution on Wings in the Lower Critical Speed Range. Transonic Aerodynamics. AGARD CP No. 35, Sept. 1968, pp. 17-1–17-10.

TABLE I.- AIRFOIL DESIGN SPECIFICATIONS

(a) Hover configuration

Parameter	Objective/ Constraint	Mach Number M	Reynolds Number R	Priority
Minimum lift coefficient $c_{l,\min}$	0.40	0.50	5.00×10^6	Medium
Maximum lift coefficient $c_{l,\max}$	1.50			High
Lower limit of low-drag, lift-coefficient range $c_{l,ll}$	0.60			Medium
Upper limit of low-drag, lift-coefficient range $c_{l,ul}$	1.40			High
Pitching-moment coefficient c_m at $c_l = 1.50$	≥ -0.10	0.40	4.00×10^6	Low
Thickness t/c	—			—
Other: Maximum lift coefficient $c_{l,\max}$ relatively independent of leading-edge roughness Docile stall characteristics at $M = 0.2$ and $R = 2.0 \times 10^6$ (i.e., verifiable in The Pennsylvania State University Low-Speed, Low-Turbulence Wind Tunnel)				

TABLE I.- Concluded

(b) Forward-flight configuration

Parameter	Objective/ Constraint	Mach Number M	Reynolds Number R	Priority
Minimum lift coefficient $c_{l,min}$	0.00	0.72	7.20×10^6	Medium
Maximum lift coefficient $c_{l,max}$	0.80	0.60	6.00×10^6	Low
Lower limit of low-drag, lift-coefficient range $c_{l,ll}$	0.02	0.70	7.00×10^6	High
Upper limit of low-drag, lift-coefficient range $c_{l,ul}$	0.10			Medium
Zero-lift pitching-moment coefficient $c_{m,0}$	≥ -0.02	0.72	7.20×10^6	High
Thickness t/c	Thickness of hover configuration			Constraint
Other: Maximum lift coefficient $c_{l,max}$ relatively independent of leading-edge roughness Drag-divergence Mach number $M_{dd} \geq 0.75$ at $c_l = 0.00$				

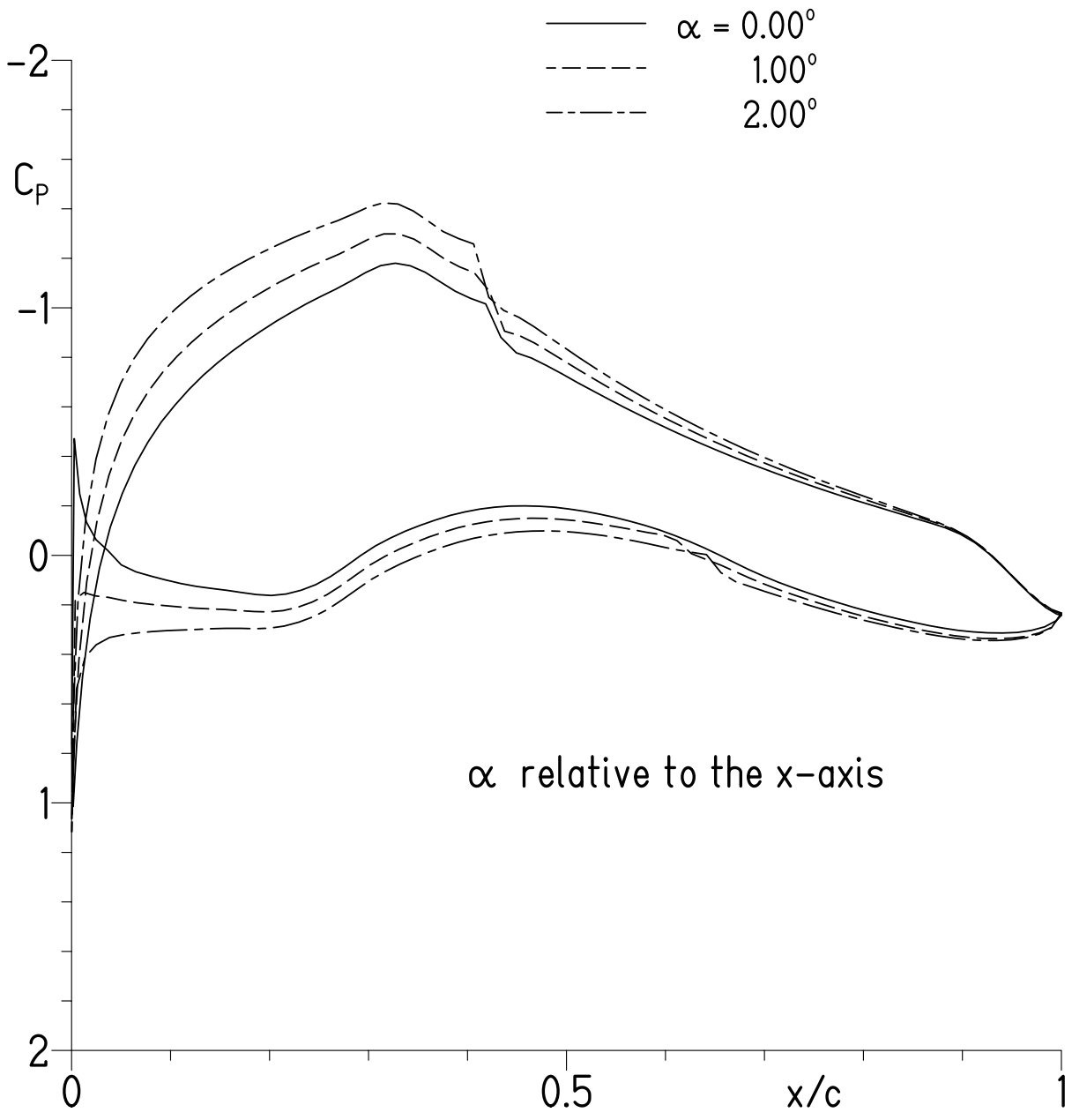

(a) $\alpha = 0.00°$, 1.00°, and 2.00°.

Figure 1.- Pressure distributions for S415 airfoil at $M = 0.50$ and $R = 5.00 \times 10^6$ with transition free.

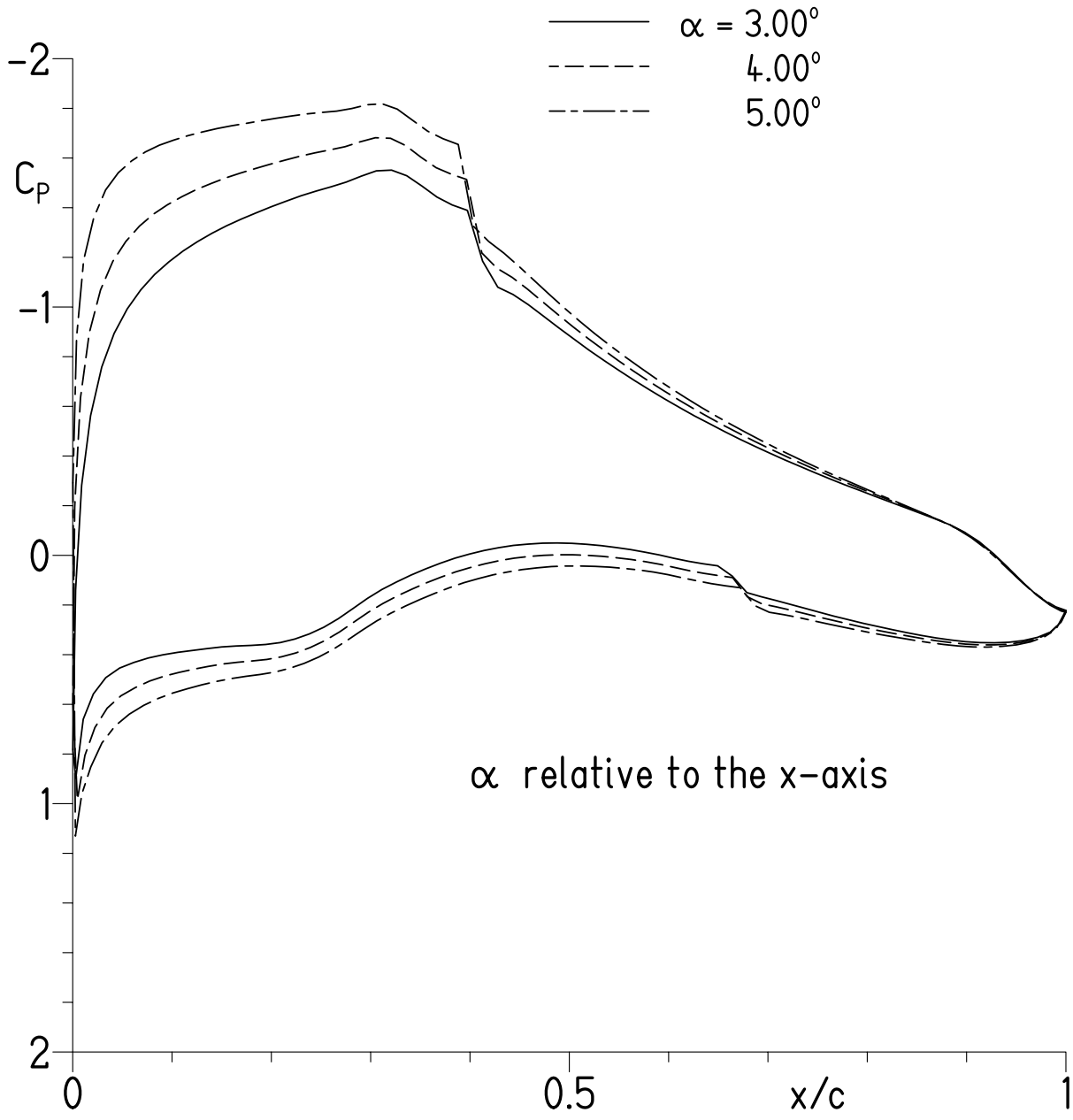

(b) $\alpha = 3.00°$, 4.00°, and 5.00°.

Figure 1.- Continued.

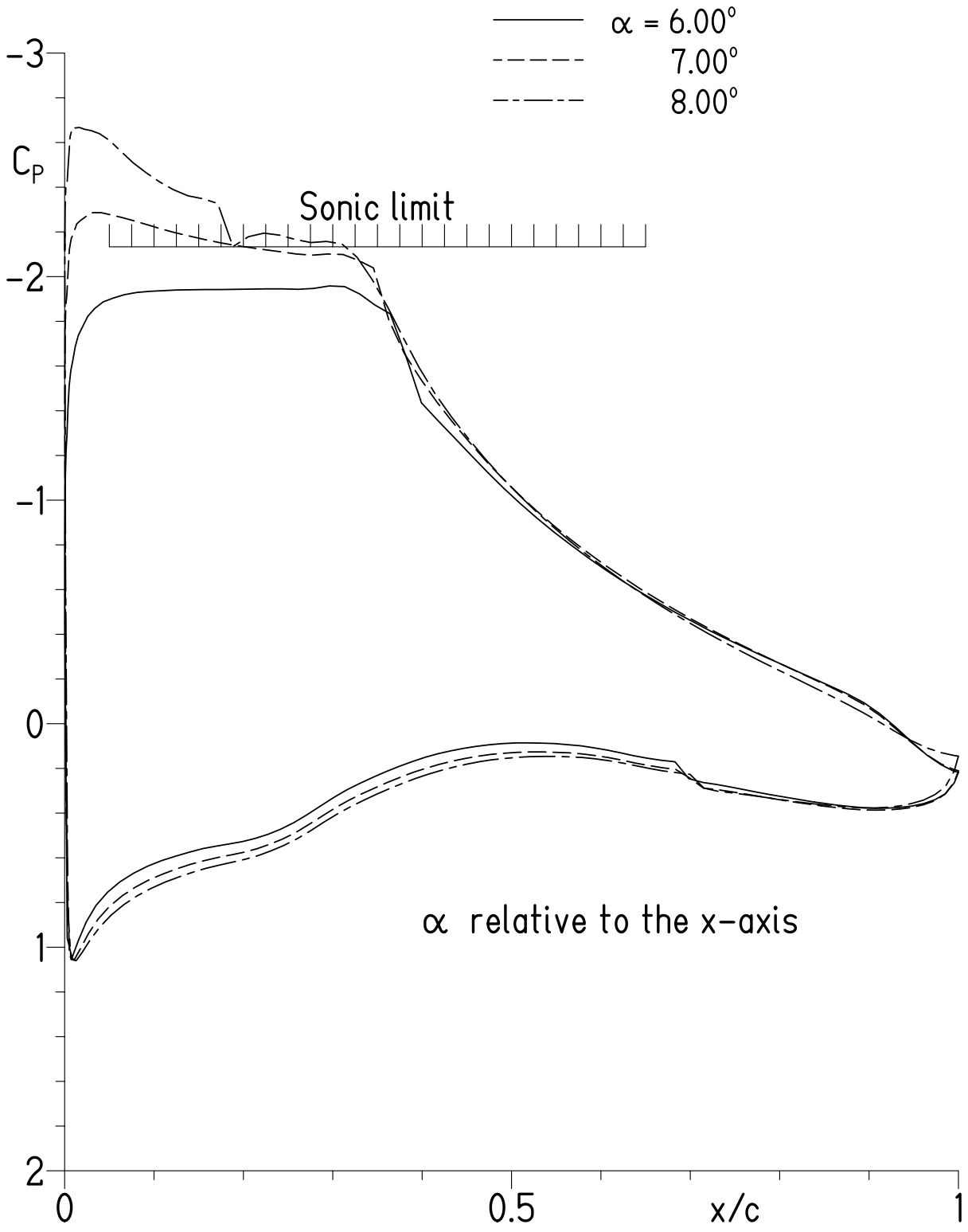

(c) $\alpha = 6.00°$, 7.00°, and 8.00°.

Figure 1.- Concluded.

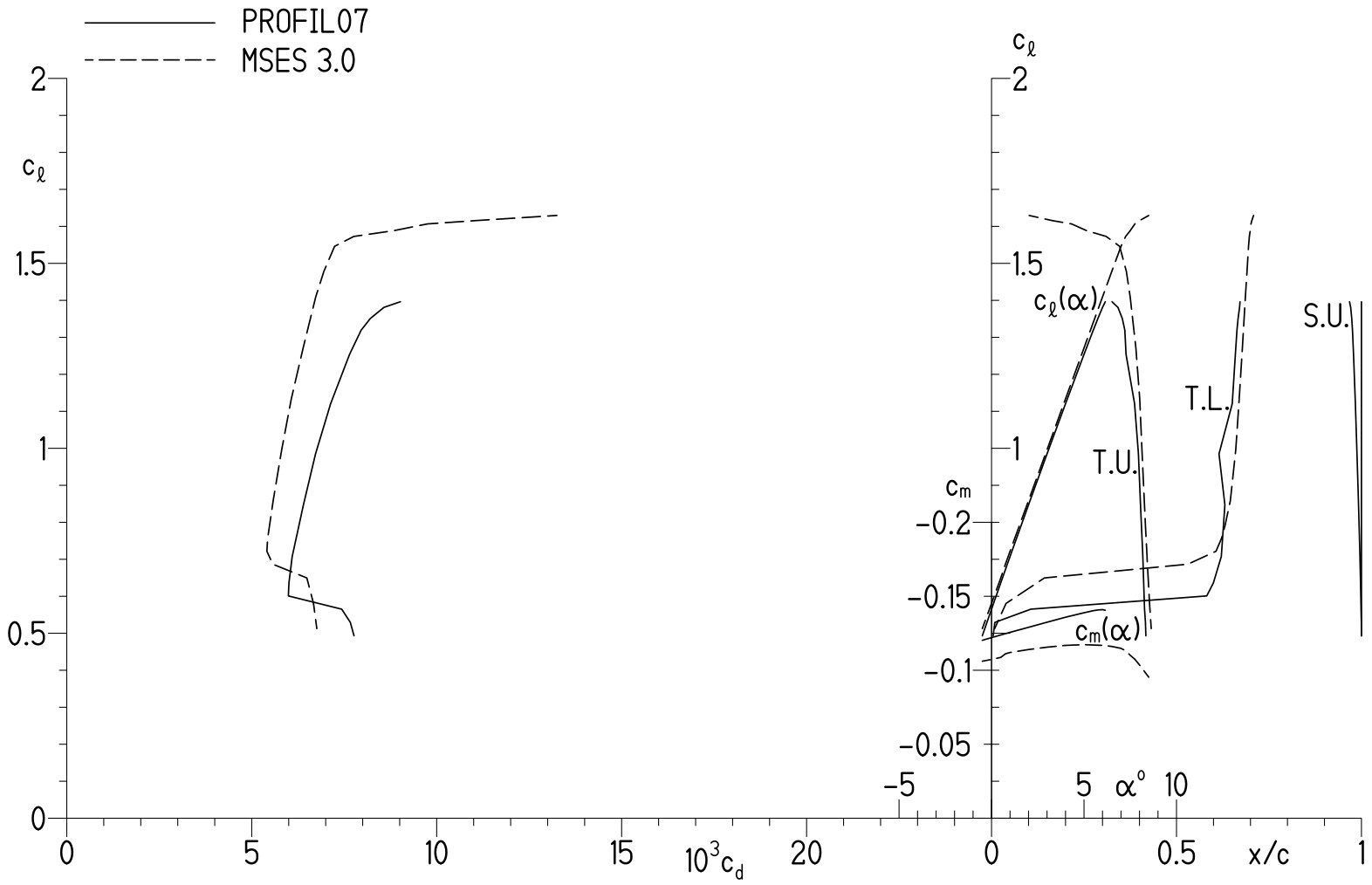

Figure 2.- Section characteristics of S415 airfoil at $M = 0.50$ and $R = 5.00 \times 10^6$ with transition free.

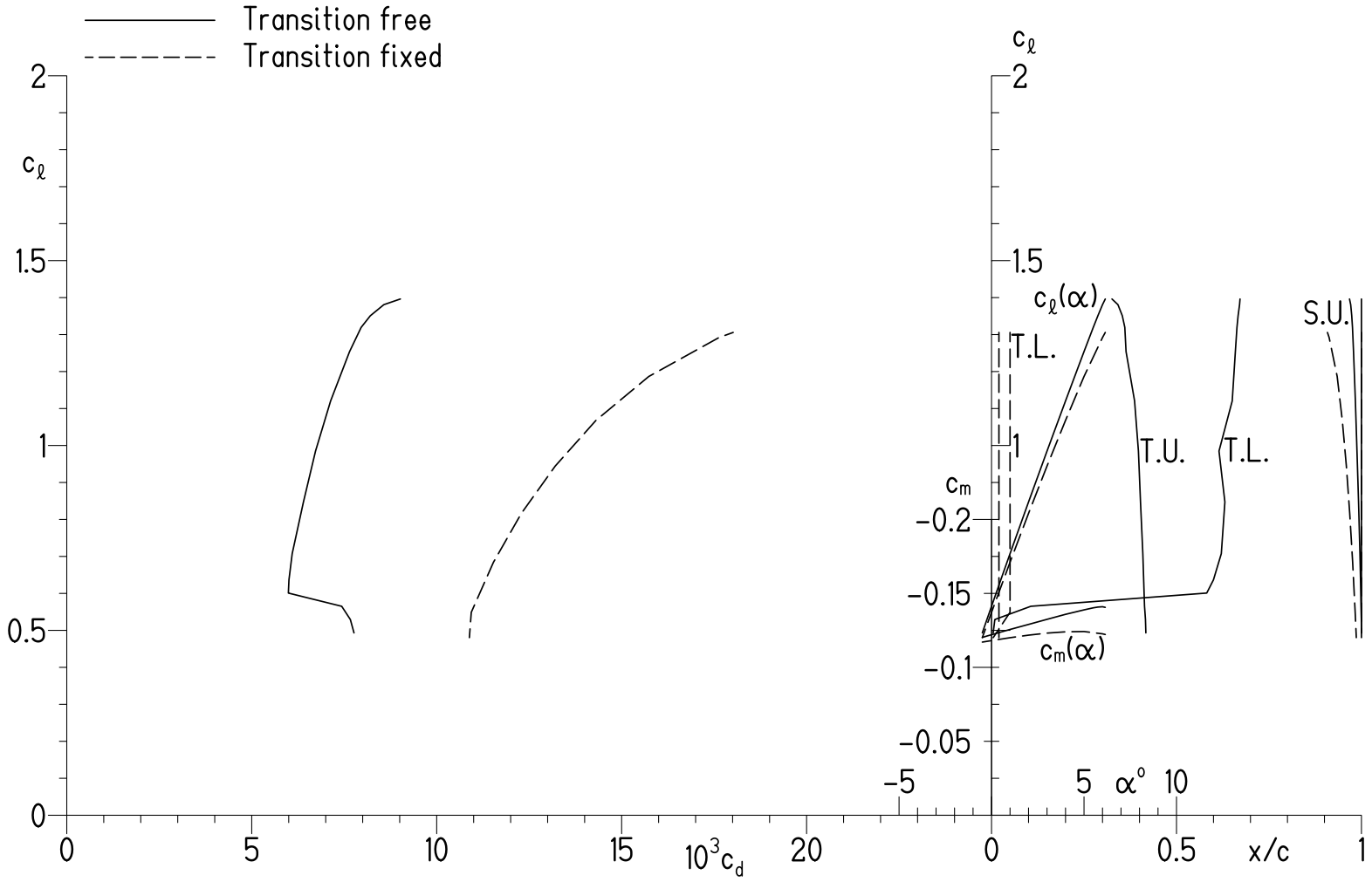

(a) PROFIL07.

Figure 3.- Effect of fixing transition on section characteristics of S415 airfoil at $M = 0.50$ and $R = 5.00 \times 10^6$.

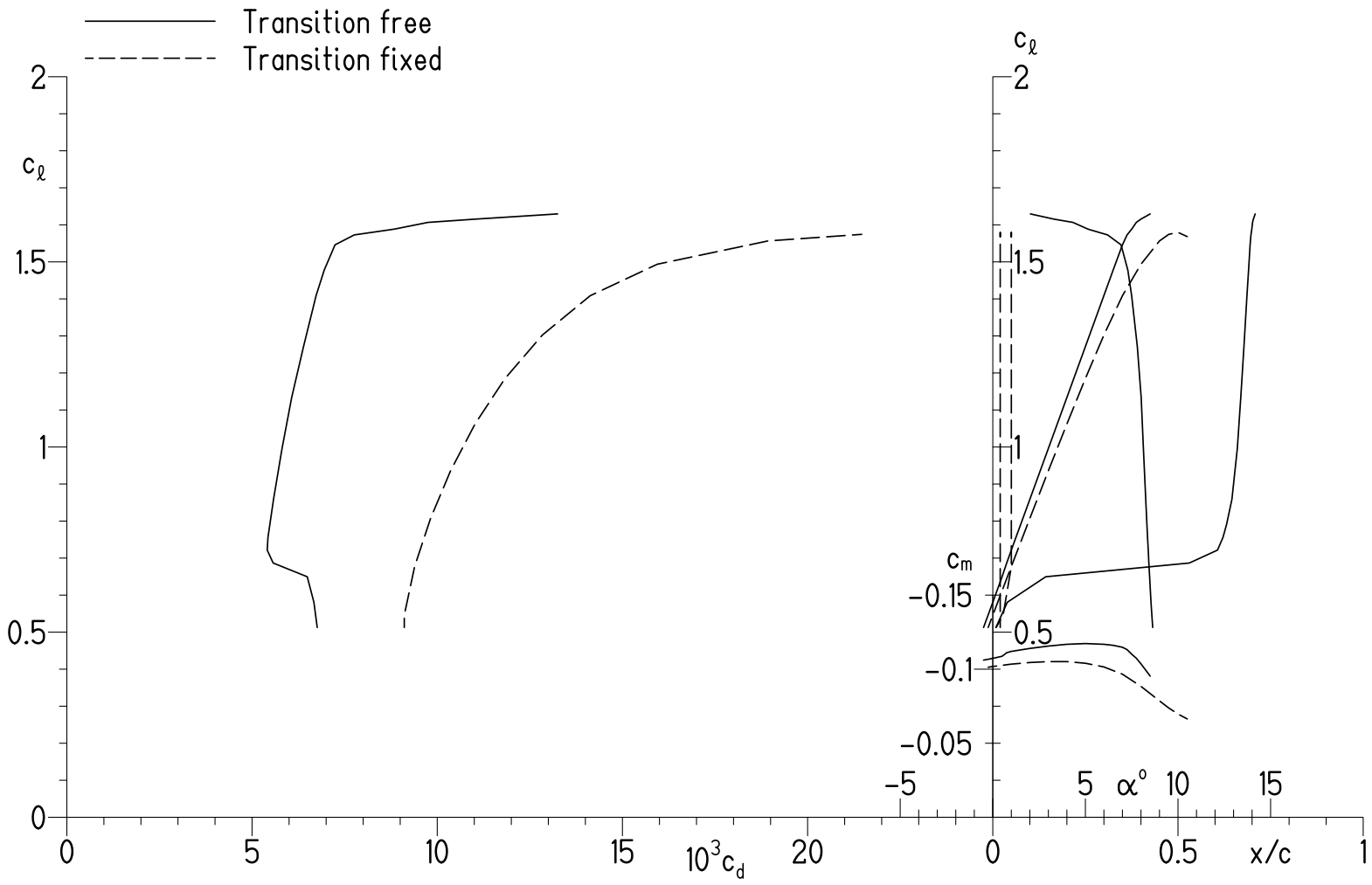

(b) MSES 3.0.

Figure 3.- Concluded.

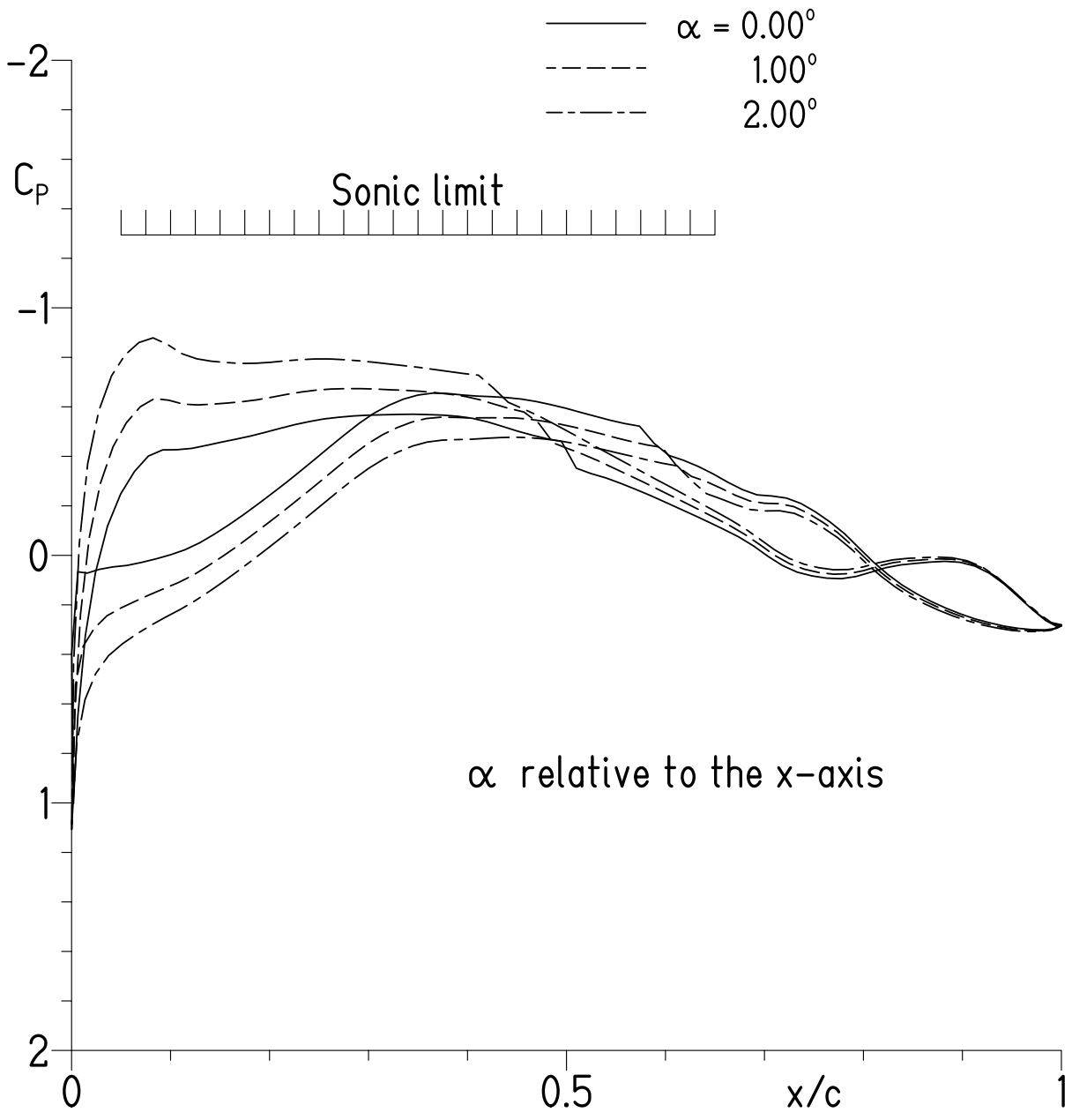

(a) $\alpha = 0.00°$, 1.00°, and 2.00°.

Figure 4.- Pressure distributions for S418 airfoil at $M = 0.60$ and $R = 6.00 \times 10^6$ with transition free.

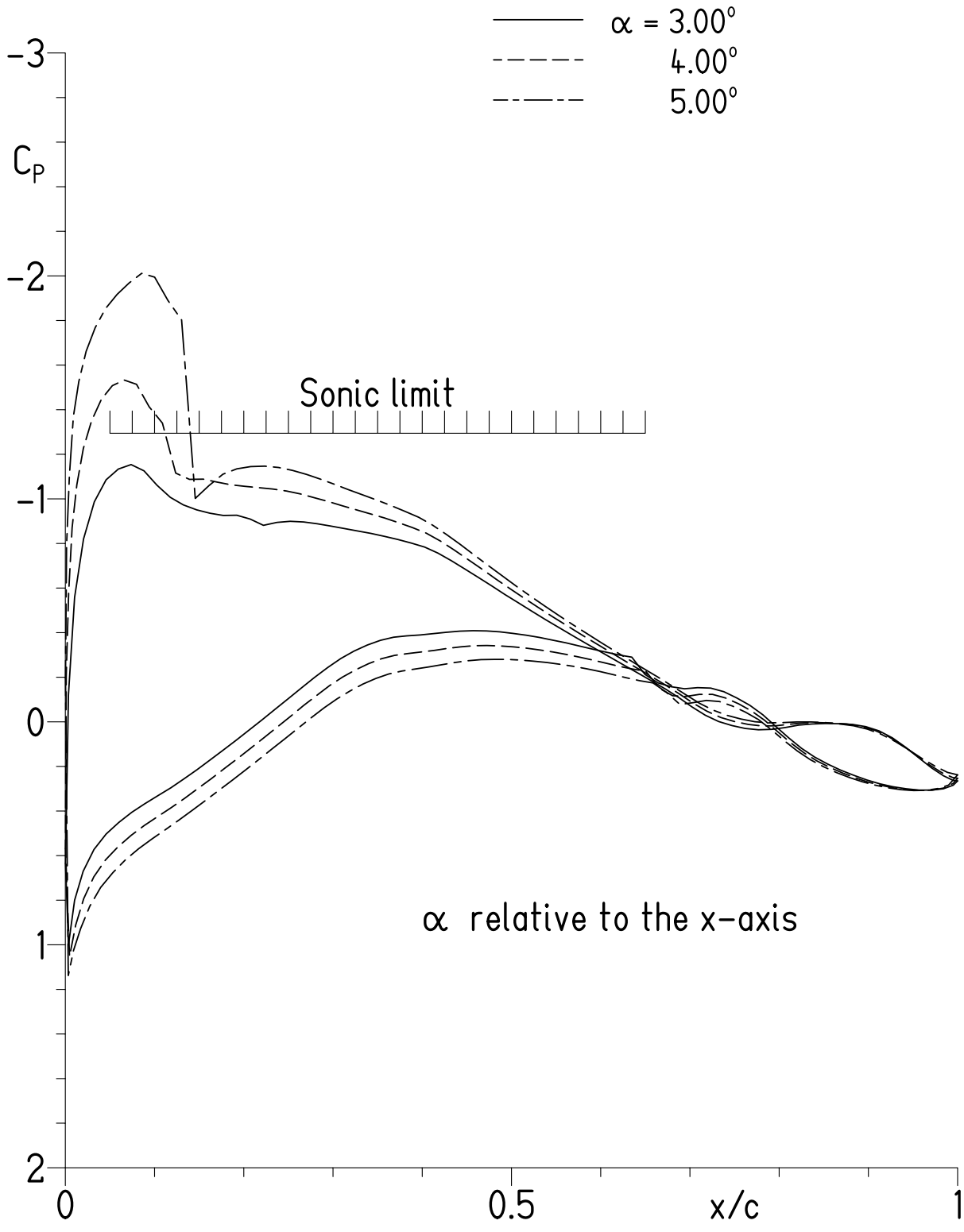

(b) $\alpha = 3.00°$, 4.00°, and 5.00°.

Figure 4.- Concluded.

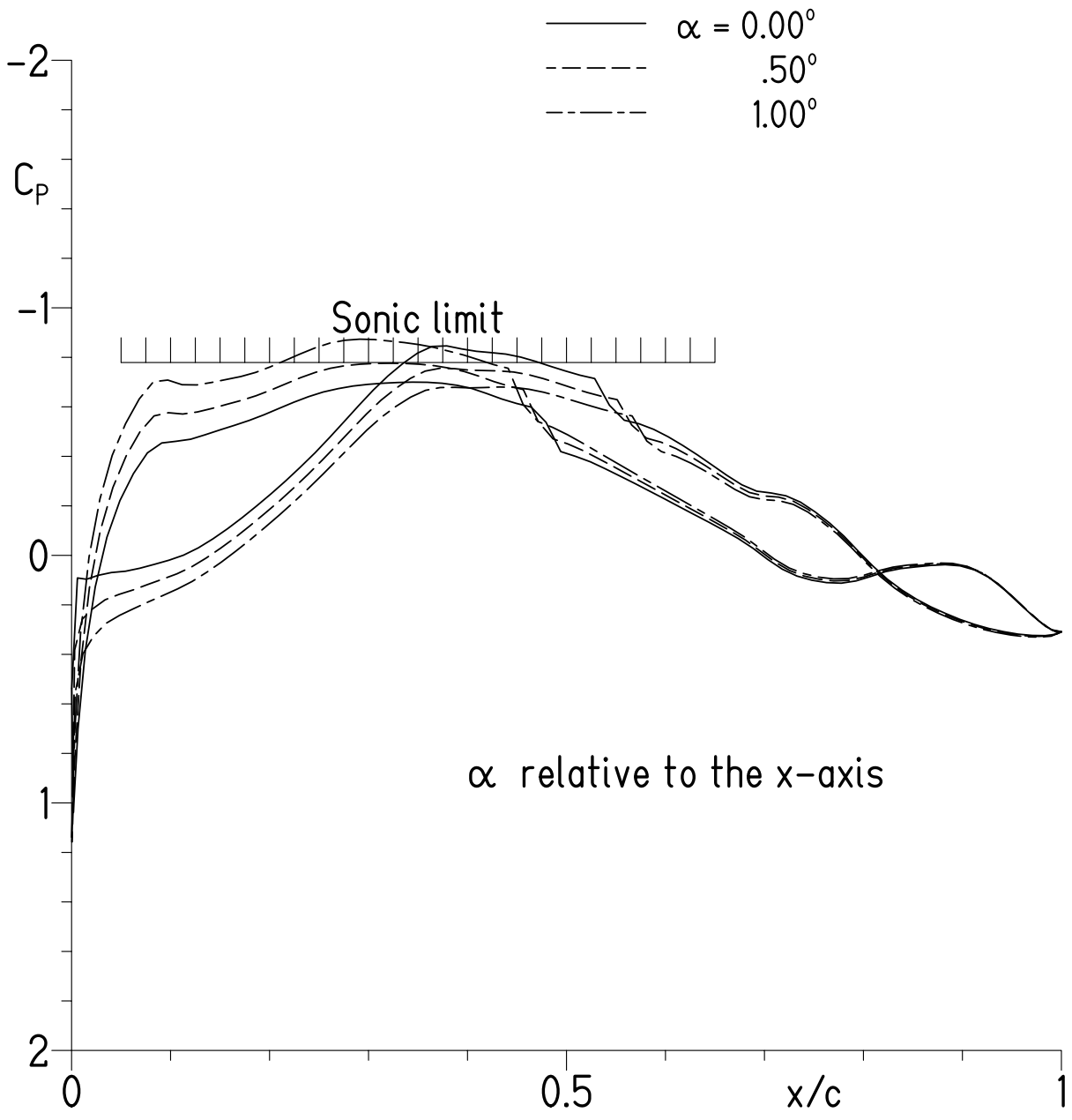

(a) $\alpha = 0.00°$, 0.50°, and 1.00°.

Figure 5.- Pressure distributions for S418 airfoil at $M = 0.70$ and $R = 7.00 \times 10^6$ with transition free.

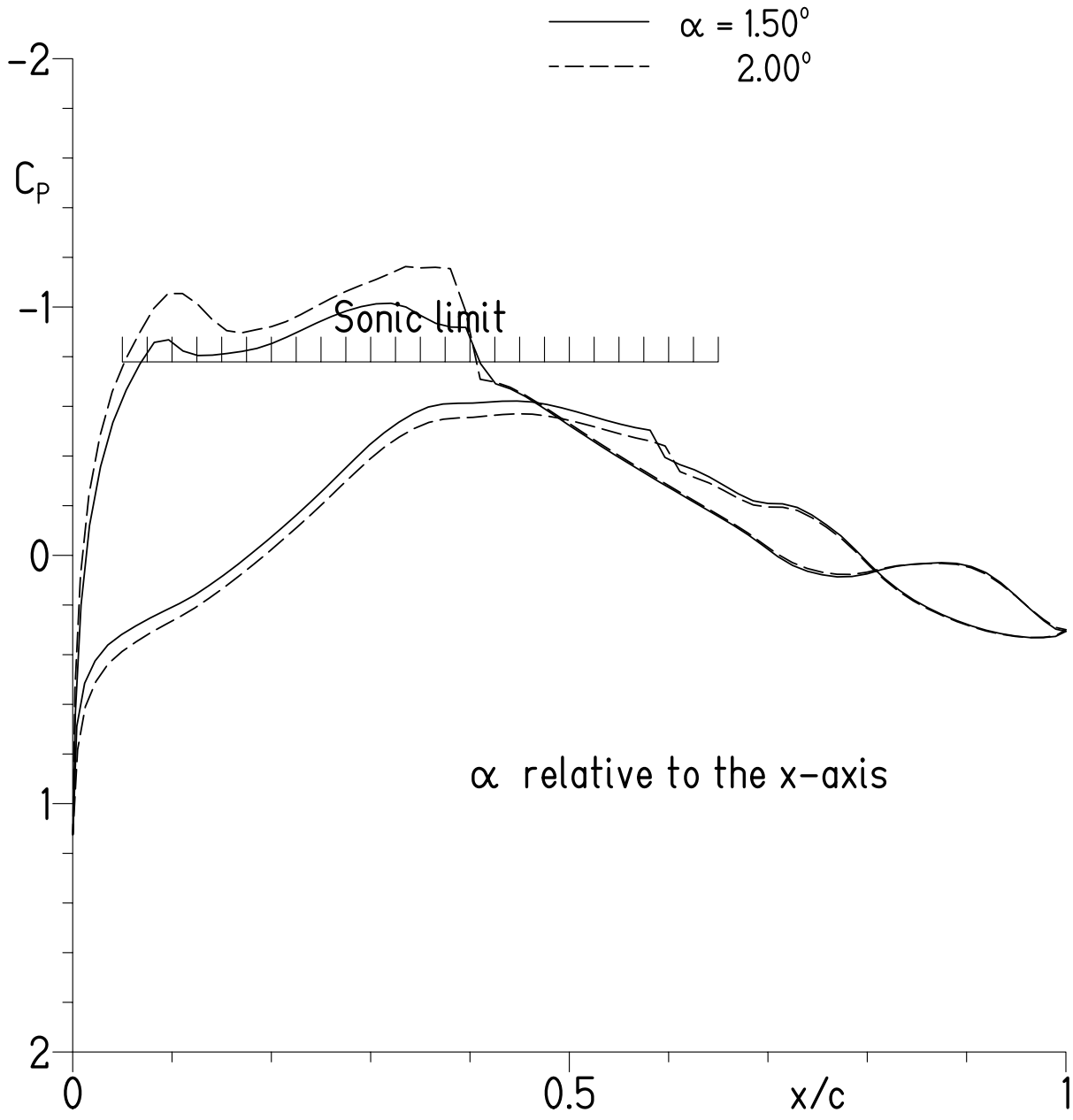

(b) $\alpha = 1.50°$ and $2.00°$.

Figure 5.- Concluded.

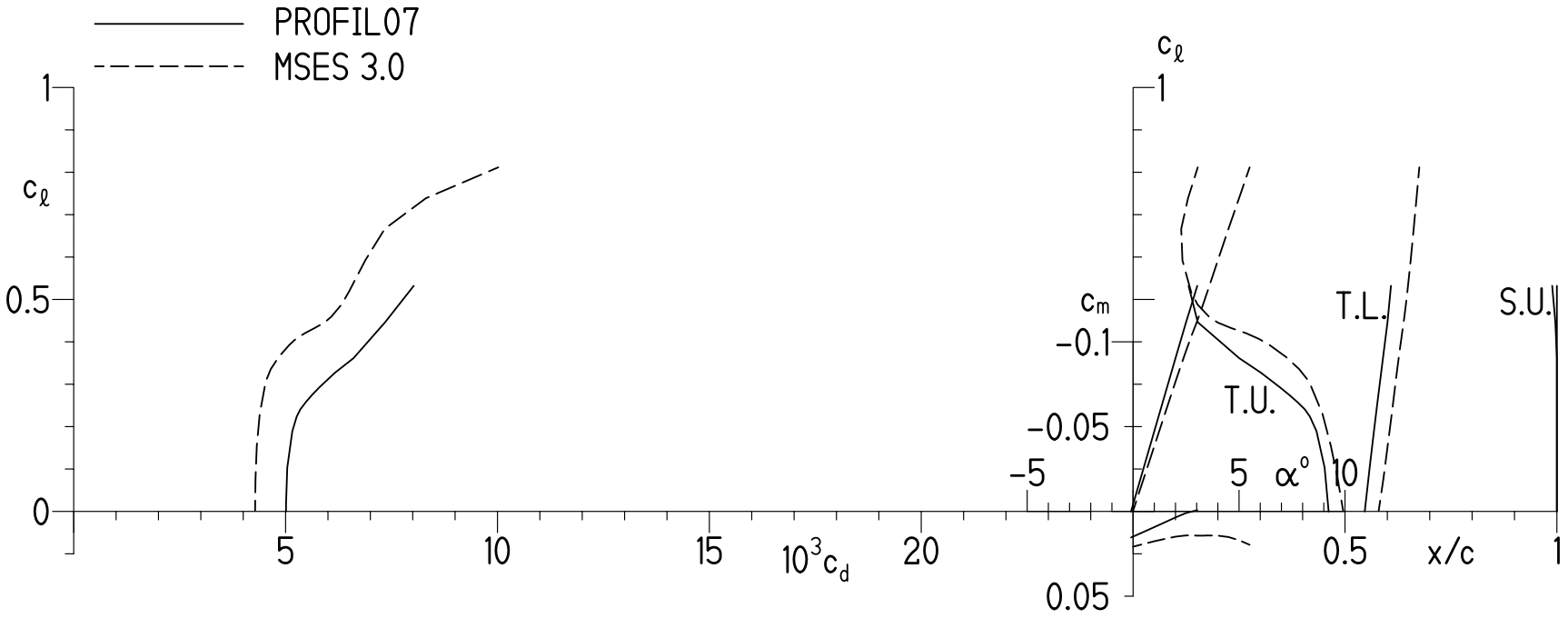

(a) M = 0.60 and R = 6.00×10^6.

Figure 6.- Section characteristics of S418 airfoil with transition free.

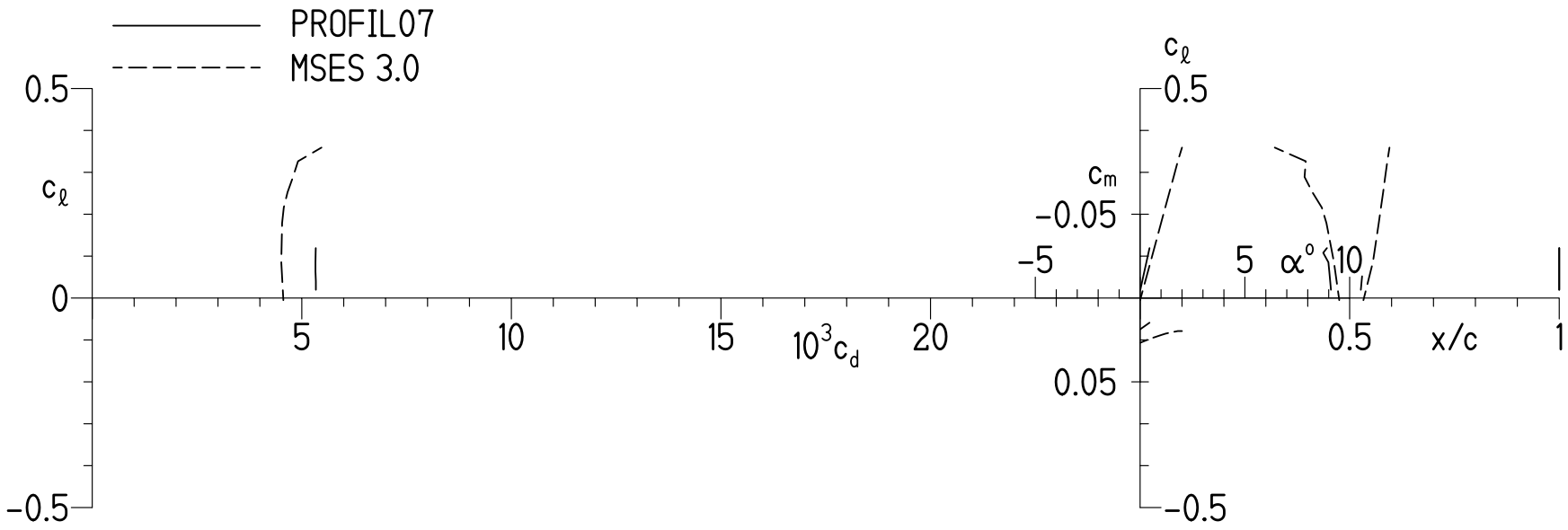

(b) M = 0.70 and R = 7.00×10^6.

Figure 6.- Concluded.

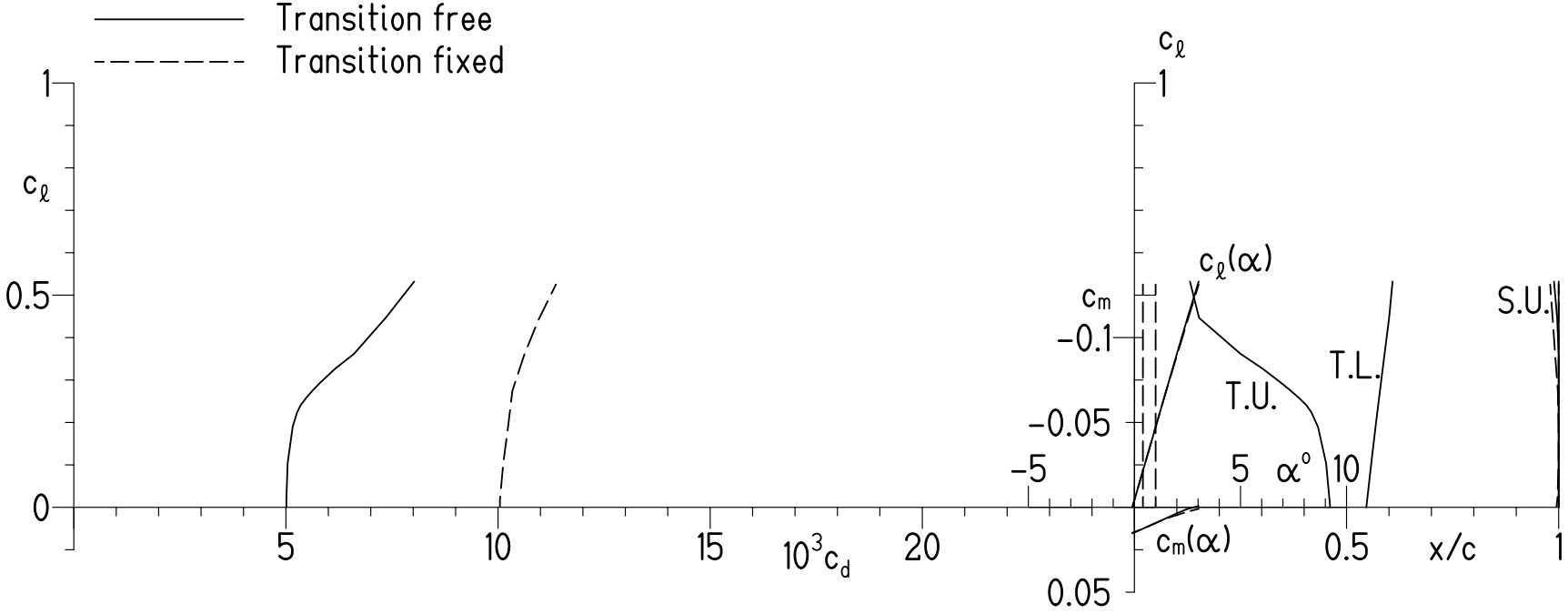

(a) PROFIL07.

Figure 7.- Effect of fixing transition on section characteristics of S418 airfoil at $M = 0.60$ and $R = 6.00 \times 10^6$.

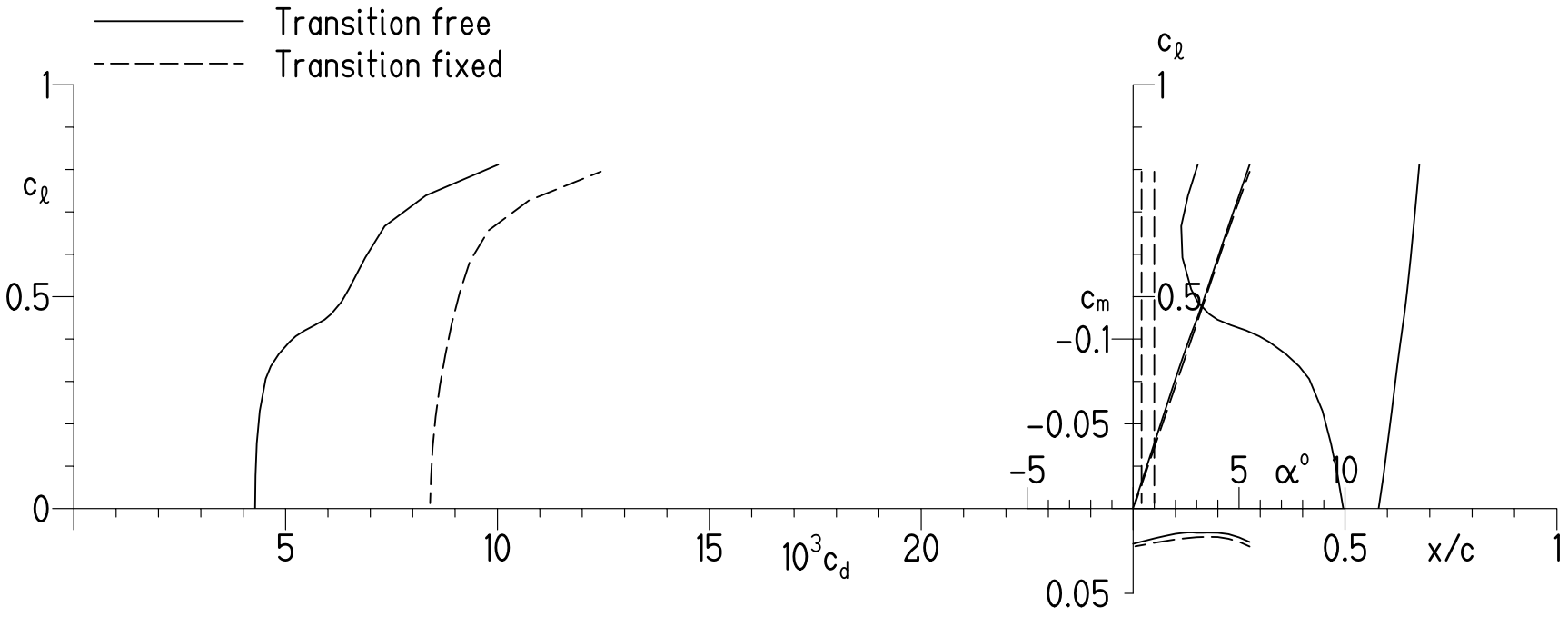

(b) MSES 3.0.

Figure 7.- Concluded.

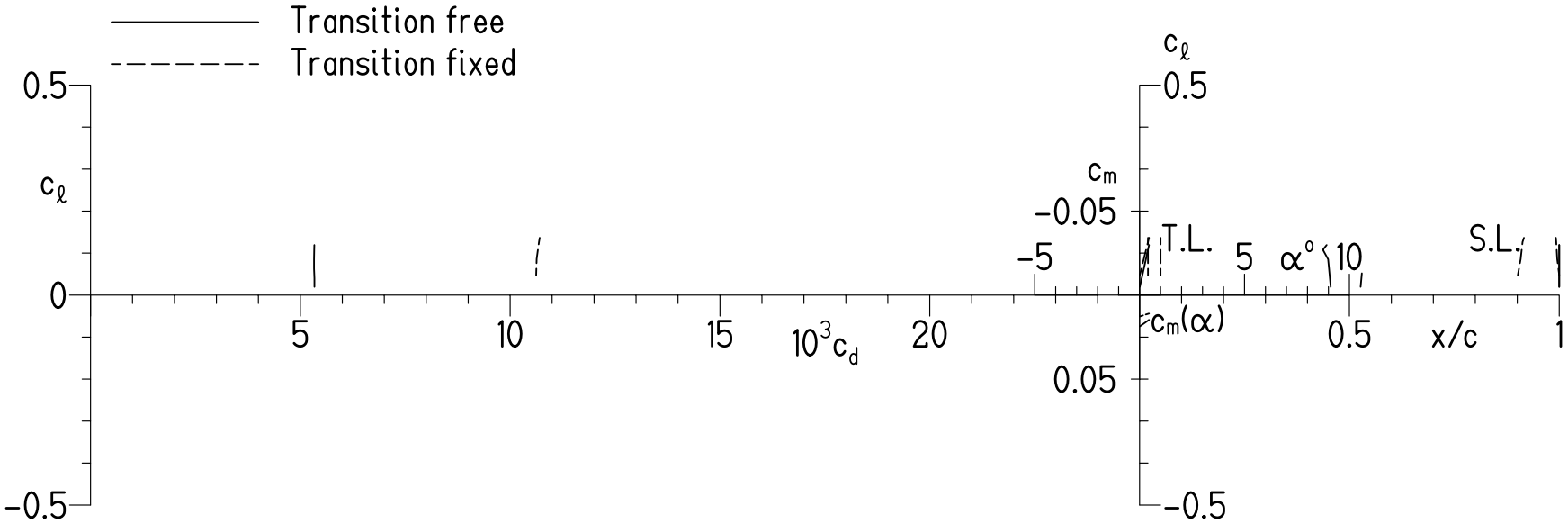

(a) PROFIL07.

Figure 8.- Effect of fixing transition on section characteristics of S418 airfoil at $M = 0.70$ and $R = 7.00 \times 10^6$.

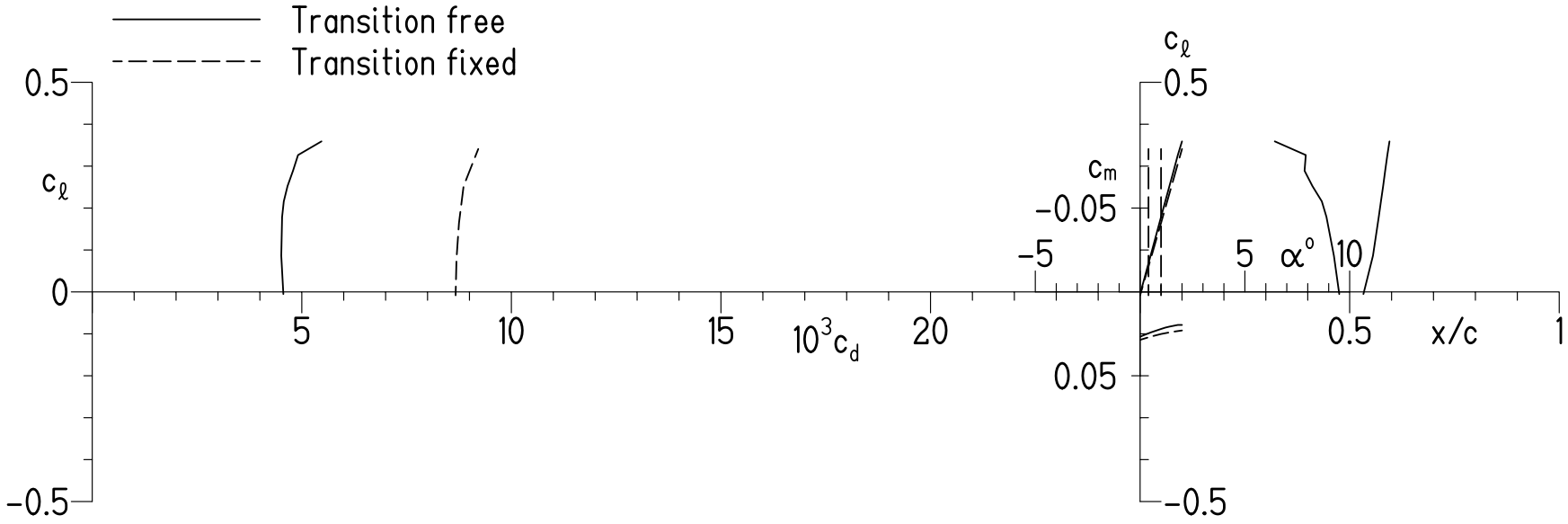

(b) MSES 3.0.

Figure 8.- Concluded.

REPORT DOCUMENTATION PAGE

Form Approved
OMB No. 0704-0188

1. REPORT DATE *(DD-MM-YYYY)*	2. REPORT TYPE	3. DATES COVERED *(From - To)*
xx 08 2010	FINAL REPORT	Sep 2007 Jun 2010

4. TITLE AND SUBTITLE

The S415 and S418 Airfoils

5a. CONTRACT NUMBER
W911W6 07 C 0047

5b. GRANT NUMBER

5c. PROGRAM ELEMENT NUMBER

6. AUTHOR(S)

Somers, Dan M.

5d. PROJECT NUMBER

5e. TASK NUMBER

5f. WORK UNIT NUMBER

7. PERFORMING ORGANIZATION NAME(S) AND ADDRESS(ES)

Airfoils, Incorporated
Attn: Dan M. Somers
122 Rose Drive
Port Matilda PA 16870 7535

8. PERFORMING ORGANIZATION REPORT NUMBER

SBIR Topic Number A06 006
Proposal Number A2 2972

9. SPONSORING / MONITORING AGENCY NAME(S) AND ADDRESS(ES)

US Army Aviation Research, Development and Engineering Command (RDECOM)
Aviation Applied Technology Directorate (AATD)
Fort Eustis VA 23604 5577

10. SPONSOR/MONITOR'S ACRONYM(S)

11. SPONSOR/MONITOR'S REPORT NUMBER(S)
RDECOM TR 10 D 113

12. DISTRIBUTION / AVAILABILITY STATEMENT

Approved for public release; distribution is unlimited.

13. SUPPLEMENTARY NOTES

UL Note: No proprietary / limited information may be included in the abstract.

14. ABSTRACT

Two, 14.1 percent thick, natural laminar flow airfoils, the S415 and S418, intended for the blade of a slowed rotor helicopter have been designed and analyzed theoretically. The S415 airfoil, designed for the hover condition, is "unmorphed" into the S418 airfoil, which is more suitable for forward flight. The two primary objectives of high maximum lift and low profile drag have been achieved. The constraints on the pitching moments have been satisfied.

15. SUBJECT TERMS

Airfoils, rotorcraft, laminar flow

16. SECURITY CLASSIFICATION OF:			17. LIMITATION OF ABSTRACT	18. NUMBER OF PAGES	19a. NAME OF RESPONSIBLE PERSON
a. REPORT	b. ABSTRACT	c. THIS PAGE			Dan M. Somers
unclassified	unclassified	unclassified	UU	29	19b. TELEPHONE NUMBER *(include area code)* (814) 357 0500